ARTICLES
https://doi.org/10.1038/s41561-019-0464-x
nature geoscience

A two-pollutant strategy for improving ozone and particulate air quality in China

Ke Li[1,2], Daniel J. Jacob[2*], Hong Liao[3*], Jia Zhu[3], Viral Shah[2], Lu Shen[2], Kelvin H. Bates[2], Qiang Zhang[4] and Shixian Zhai[2]

Fine particulate matter ($PM_{2.5}$) decreased by 30–40% across China during 2013–2017 in response to the governmental Clean Air Action. However, surface ozone pollution worsened over the same period. Model simulations have suggested that the increase in ozone could be driven by the decrease in $PM_{2.5}$, because $PM_{2.5}$ scavenges hydroperoxy (HO_2) and NO_x radicals that would otherwise produce ozone. Here we show observational evidence for this effect with 2013–2018 summer data of hourly ozone and $PM_{2.5}$ concentrations from 106 sites in the North China Plain. The observations show suppression of ozone pollution at high $PM_{2.5}$ concentrations, consistent with a model simulation in which $PM_{2.5}$ scavenging of HO_2 and NO_x depresses ozone concentrations by 25 ppb relative to $PM_{2.5}$-free conditions. $PM_{2.5}$ chemistry makes ozone pollution less sensitive to NO_x emission controls, emphasizing the need for controlling emissions of volatile organic compounds (VOCs), which so far have not decreased in China. The new 2018–2020 Clean Air Action plan calls for a 10% decrease in VOC emissions that should begin to reverse the long-term ozone increase even as $PM_{2.5}$ continues to decrease. Aggressive reduction of NO_x and aromatic VOC emissions should be particularly effective for decreasing both $PM_{2.5}$ and ozone.

China is confronting serious air pollution, with surface air concentrations of fine particulate matter ($PM_{2.5}$) and ozone routinely exceeding air quality standards[1–3]. In 2013, the Chinese government introduced a 5 yr (2013–2017) plan for Clean Air Action[4]. The plan targeted $PM_{2.5}$ as the most urgent threat to public health[5], and it principally focused emission controls on primary particles and sulfur dioxide (SO_2) from coal combustion. As a result, $PM_{2.5}$ concentrations across urban areas of China decreased by 30–40% during 2013–2017 (ref. [6]). At the same time, however, surface ozone concentrations increased[1,7]. Annual mortality attributable to surface ozone pollution in China is at present over 50,000 deaths according to ref. [3] and 154,000–316,000 deaths according to ref. [8]. Ozone pollution is also detrimental to vegetation[9], crop yields[10] and building materials[11].

Surface ozone is produced rapidly in polluted air by photochemical oxidation of volatile organic compounds (VOCs) catalysed by nitrogen oxide radicals ($NO_x \equiv NO + NO_2$) and hydrogen oxide radicals ($HO_x \equiv OH + HO_2 +$ organic peroxy radicals (RO_2)). VOCs and NO_x are emitted mainly from fuel combustion and industrial sources[12], and biogenic sources also contribute to VOC emissions[13]. HO_x originates mainly from photochemical oxidation of water vapour and photolysis of carbonyls[14], so ozone pollution is generally worst in summer. Summer ozone pollution is particularly severe over urbanized eastern China, with most sites from the Ministry of Ecology and Environment (MEE) network far exceeding the 8 h daily maximum (MDA8) air quality standard of 82 ppb (refs. [1,13,15]). The chemistry involved in ozone formation is highly nonlinear and may be limited by the supply of either NO_x or VOCs, which has implications for which sources to control[16,17]. Satellite observations of the ratio of formaldehyde (HCHO) to nitrogen dioxide (NO_2) in the atmospheric column suggest that urban regions of China are in a transition regime between NO_x-limited and VOC-limited, while rural areas are NO_x-limited[18]. However, ozone production in urban centres is thought to be VOC-limited[13].

In previous work[15], we showed that the 2013–2017 ozone increase in China was of anthropogenic rather than meteorological origin. According to the Multiresolution Emission Inventory for China (MEIC)[12], anthropogenic NO_x emissions in China decreased by 20% during 2013–2017, while VOC emissions increased by 2%. These emission trends alone cannot explain the increase in ozone. Using simulations from the Goddard Earth Observing System Chemical Transport Model (GEOS-Chem), we suggested that the ozone increase could instead be driven by the $PM_{2.5}$ decrease, due to the role of $PM_{2.5}$ as scavenger of hydroperoxy (HO_2) radicals that would otherwise react with nitric oxide (NO) to produce ozone. Here we demonstrate this ozone–$PM_{2.5}$ linkage with MEE network observations during pollution episodes, and we show that it affects whether ozone production is limited by the supply of NO_x or VOCs. The results have important implications for developing two-pollutant control strategies to decrease both $PM_{2.5}$ and ozone in China.

Observed ozone–$PM_{2.5}$ relationship

Figure 1a shows the ozone–$PM_{2.5}$ relationship in daily summer observations of MDA8 ozone and 24 h $PM_{2.5}$ concentrations at sites operated by the MEE during 2013–2018. We focus on the four megacity clusters targeted by the 2013–2017 Clean Air Action: North China Plain (106 sites), Yangtze River Delta (84 sites), Pearl River Delta (66 sites) and Sichuan Basin (71 sites). We averaged the daily MDA8 ozone and $PM_{2.5}$ data over all sites in a given cluster to obtain the daily time series, removed the 2013–2018 trends (Methods) to avoid the influence from the $PM_{2.5}$ concentration decrease over the period and binned the data into 5 $\mu g\,m^{-3}$ $PM_{2.5}$ increments.

[1]Harvard-NUIST Joint Laboratory for Air Quality and Climate, Nanjing University of Information Science and Technology, Nanjing, China. [2]Harvard John A. Paulson School of Engineering and Applied Sciences, Harvard University, Cambridge, MA, USA. [3]Jiangsu Key Laboratory of Atmospheric Environment Monitoring and Pollution Control, Collaborative Innovation Center of Atmospheric Environment and Equipment Technology, School of Environmental Science and Engineering, Nanjing University of Information Science and Technology, Nanjing, China. [4]Department of Earth System Science, Tsinghua University, Beijing, China. *e-mail: djacob@fas.harvard.edu; hongliao@nuist.edu.cn

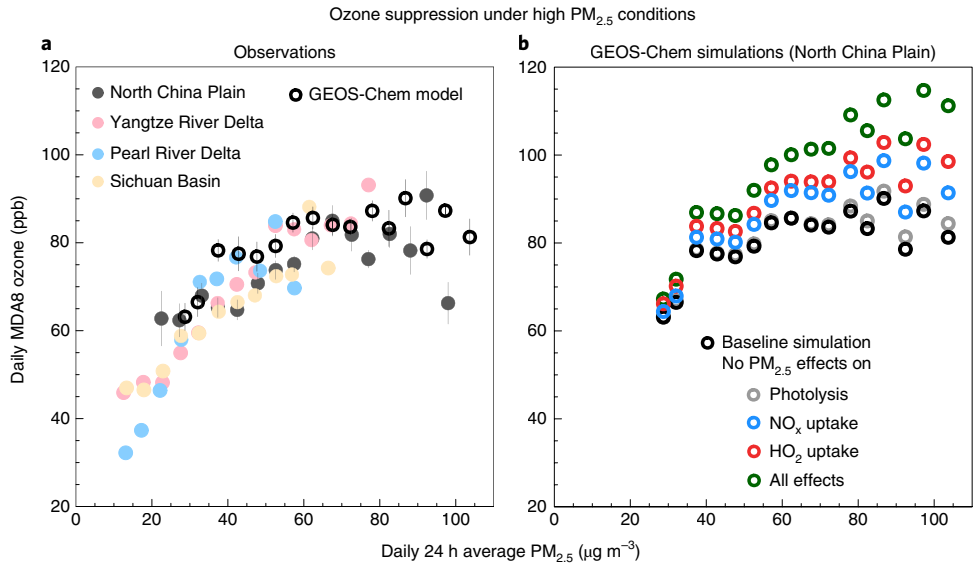

Fig. 1 | Ozone–$PM_{2.5}$ relationship in China in summer. a, Observed 2013–2018 relationships in daily data for MDA8 ozone and 24 h average $PM_{2.5}$ concentrations. Values are regional averages over 5 μg m^{-3} $PM_{2.5}$ bins (at least three data points required) for the monitoring sites operated by China's MEE in the four megacity clusters targeted by the Clean Air Action (see Methods for geographical definitions): North China Plain, Yangtze River Delta, Pearl River Delta and Sichuan Basin. Multi-year trends (2013–2018) of ozone and $PM_{2.5}$ have been removed (Methods) to avoid obfuscating influence from the large $PM_{2.5}$ decrease over the period (see Supplementary Fig. 5 for the relationships in the non-detrended data). GEOS-Chem simulation results for the North China Plain (2016–2017) are also shown. Error bars shown for the North China Plain are standard errors of ozone concentrations for each bin. **b**, GEOS-Chem baseline simulation for the North China Plain (as in **a**) and sensitivity simulations removing the effects of $PM_{2.5}$ on photolysis rates, NO_x uptake and HO_2 uptake, first separately and then together.

We see in Fig. 1a a generally positive correlation between daily MDA8 ozone and $PM_{2.5}$, which is consistent across the four megacity clusters. This positive correlation is typical of summer observations in polluted regions[19,20]. It can be understood as reflecting common dependences of ozone and $PM_{2.5}$ on meteorology, manifested in particular by strong correlations of both with temperature and wind speed[6,15]. The North China Plain has particularly high $PM_{2.5}$, frequently exceeding 60 μg m^{-3}. There we find that ozone levels off at about 80 ppb even as $PM_{2.5}$ increases to about 100 μg m^{-3}. As shown in Fig. 1a, a GEOS-Chem model simulation (Methods) conducted for 2016–2017 and sampled in the same way as the observations closely reproduces this behaviour.

The levelling off of ozone under highly polluted conditions might simply reflect the relatively short ozone lifetime against sinks from deposition and chemistry[21] or the self-suppression of ozone production as the NO/NO_2 ratio shifts towards NO_2 with increasing ozone. To isolate the role of $PM_{2.5}$, we conducted a GEOS-Chem sensitivity simulation removing $PM_{2.5}$ effects on chemistry and photolysis (Fig. 1b). We find in that simulation that ozone does not level off until it reaches about 110 ppb. For polluted conditions with $PM_{2.5}$ exceeding 80 μg m^{-3}, we see from Fig. 1b that $PM_{2.5}$ effects are responsible for about a 25 ppb suppression of ozone relative to $PM_{2.5}$-free conditions. This is a much larger effect than previously reported by ref. [15], which did not focus on pollution episodes.

We conducted further sensitivity simulations in the model to isolate the contributions from different $PM_{2.5}$ effects on ozone (Methods). For the days with $PM_{2.5}$ exceeding 80 μg m^{-3} in Fig. 1b, we find that not including individual $PM_{2.5}$ effects on photolysis rates, NO_x uptake and HO_2 uptake increases ozone on average by 2 ppb, 9 ppb and 15 ppb, respectively. The small effect from photolysis is consistent with previous model simulations[22,23]. Changes in atmospheric dynamics through aerosol–radiation interactions are not considered in our work but increase ozone by less than 2 ppb in the aforementioned model simulations[22].

The largest effect of $PM_{2.5}$ on ozone is through HO_2 uptake, as reported in our previous work[15]. This uptake provides a sink for HO_x radicals and hence suppresses ozone formation. There is considerable evidence in the literature for HO_2 uptake by particles with a reactive uptake coefficient γ_{HO_2} in the range 0.1–1.0 (refs. [24–26]). Our GEOS-Chem simulations use $\gamma_{HO_2} = 0.2$ with hydrogen peroxide (H_2O_2) as product, as recommended by ref. [24]. Ref. [26] recommends $\gamma_{HO_2} = 0.24$ based on their ensemble of measurements for aerosol samples collected at two mountain sites in eastern China, showing consistent HO_2 uptake with no apparent dependence on $PM_{2.5}$ composition. There is uncertainty as to whether the product of HO_2 uptake is H_2O_2 or H_2O (ref. [27]), but this has little effect on our ozone simulation[15].

The effect of NO_x uptake by $PM_{2.5}$ involves aqueous-phase conversion of NO_2, nitrate radical (NO_3) and dinitrogen pentoxide (N_2O_5) to nitric acid (HNO_3) (ref. [24]). Here we updated the reactive uptake coefficients for these reactions in GEOS-Chem following ref. [28] (Methods). The effect of NO_x uptake on ozone is larger than previously reported by ref. [15] for 2013 conditions, and this is partly due to the 20% decrease in NO_x emissions since then, which has made ozone production more NO_x sensitive (Supplementary Fig. 1).

$PM_{2.5}$ impact on emission control strategies for ozone

A critical issue in developing an emission control strategy for ozone pollution is to understand the relative benefits of NO_x and VOC emission controls. This is generally framed in terms of whether ozone production is NO_x-limited or VOC-limited, which depends on the dominant HO_x loss pathways[29]. In standard gas-phase mechanisms, ozone production is NO_x-limited if the dominant HO_x sink is the self-reaction of peroxy radicals to produce peroxides, and VOC-limited if the dominant HO_x sink is the reaction of NO_2 with OH to produce HNO_3. In urban areas of China, however, we find that the dominant sink is HO_2 uptake by $PM_{2.5}$, as illustrated in Fig. 2 for the North China Plain. By analogy with gas-phase formation of peroxides, one might expect this sink to push ozone production

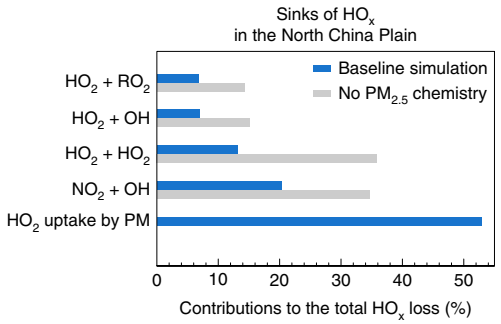

Fig. 2 | HO_x radical sinks in the North China Plain. Relative contributions of different chemical pathways to the total sink of HO_x radicals in the GEOS-Chem simulation for the boundary layer (surface to 1.3 km) over the North China Plain (114°–118° E, 34°–40° N). Results are summer 2017 averages from the baseline simulation and from a sensitivity simulation with no $PM_{2.5}$ chemistry (grey).

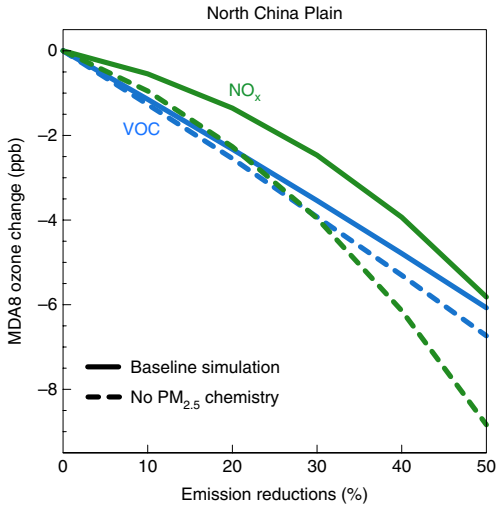

Fig. 3 | Response of mean summer MDA8 surface ozone concentrations in the North China Plain to reductions in NO_x and VOC emissions relative to 2017 levels. Results are from the baseline simulation including $PM_{2.5}$ chemistry (solid lines) and from a sensitivity simulation without $PM_{2.5}$ chemistry (dashed lines).

towards NO_x-limited conditions. NO_x uptake by $PM_{2.5}$ would do the same. However, uptake of HO_2 decreases the HO_2/OH ratio and a lower supply of HO_x radicals lengthens the lifetime of NO_x, which causes the NO_2 + OH reaction to account for a greater contribution to the HO_x sink[30,31]. Indeed, Fig. 2 shows a greater contribution of the NO_2 + OH reaction relative to gas-phase formation of peroxides ($HO_2 + HO_2$ and $RO_2 + HO_2$) when $PM_{2.5}$ chemistry is included.

To clarify this issue, we conducted simulations with uniform 10%, 20%, 30%, 40% and 50% decreases of anthropogenic NO_x or VOC emissions relative to 2017 values with and without $PM_{2.5}$ chemistry. Figure 3 shows the response for mean MDA8 ozone concentrations over the North China Plain. $PM_{2.5}$ chemistry weakens the ozone response to decreases of either NO_x or VOC emissions because of the lower concentrations of HO_x radicals. The effect is much larger for NO_x than for VOCs, because HO_2 uptake drives a net increase in NO_x concentrations as a result of lower OH concentrations and hence slower conversion to HNO_3 by the NO_2 + OH reaction (Supplementary Fig. 2). As a result, ozone production becomes more strongly VOC-limited (Fig. 3). The shift to more VOC-limited conditions because of HO_2 uptake by $PM_{2.5}$ also holds for the other megacity clusters, even though their $PM_{2.5}$ concentrations are lower (Supplementary Fig. 3).

Chemical indicators are often used in observations and models to diagnose whether ozone production is NO_x-limited or VOC-limited[32]. A frequently used indicator is the H_2O_2/HNO_3 concentration ratio[32,33], which tracks the prevailing HO_x sink. But this can be misleading if $PM_{2.5}$ is the major HO_x sink, as is the case here, particularly if the product of $PM_{2.5}$ uptake is H_2O_2. In that case, $PM_{2.5}$ chemistry causes the H_2O_2/HNO_3 ratio to increase (Supplementary Fig. 4), whereas ozone production in fact becomes more VOC-limited. The alternative indicators of the HCHO/NO_2 column concentration ratio, derived from satellite data[18,34], and the ozone/NO_y concentration ratio[35] (NO_y referring to the sum of NO_x and its oxidation products) are more robust, as shown in Supplementary Fig. 4.

Towards a joint ozone–$PM_{2.5}$ air pollution control strategy

The effect of $PM_{2.5}$ chemistry on ozone production has important implications for a coordinated emission control strategy to decrease both $PM_{2.5}$ and ozone. There is strong impetus for continuing to decrease $PM_{2.5}$ levels in China, as present-day levels still greatly exceed the air quality standard[1,6]. $PM_{2.5}$ decreases over the 2013–2017 period were driven mostly by emission controls on SO_2 and primary particles from coal combustion[12]. Data for the North China Plain indicate that organic and nitrate components of $PM_{2.5}$ are now more important than sulfate[36–38]. As leverage from decreasing SO_2 emissions diminishes, decreasing VOC and NO_x emissions may become relatively more effective for decreasing $PM_{2.5}$. Decreasing VOC and NO_x emissions would also have benefits for ozone to offset the ozone penalty from decreasing $PM_{2.5}$.

The recent 2018–2020 Clean Air Action plan calls for an 18% national decrease in $PM_{2.5}$ concentrations in 2020 relative to 2015, a 15% decrease in NO_x and SO_2 emissions and a 10% decrease in VOC emissions[39]. Taking into account the already realized 2015–2017 decreases in NO_x and SO_2 emissions[12] and in $PM_{2.5}$ concentrations[6], the remaining reduction target for 2018–2020 is 9% for NO_x emissions, 10% for VOC emissions and 8% for $PM_{2.5}$ concentrations. We applied the GEOS-Chem simulation for 2017 to examine the effects of these reductions, first separately and then together, on ozone pollution in the North China Plain. Results in Fig. 4 show that further decreases of $PM_{2.5}$ alone cause continuing ozone increases but that this is offset by the planned decreases of NO_x and VOC emissions, resulting in a small overall net benefit for ozone of about 1 ppb. This ozone benefit is similar for relatively clean (low $PM_{2.5}$) and highly polluted (high $PM_{2.5}$) conditions. Although the ozone penalty from decreasing $PM_{2.5}$ is largest under highly polluted conditions, the benefit from decreasing VOC emissions is also largest under those conditions. Larger VOC reductions than the 10% planned under the 2018–2020 Clean Air Action would provide larger ozone benefits, as illustrated in Fig. 3.

NO_x and VOC emission controls improve not only ozone but also $PM_{2.5}$. Nitrate and organic components contribute 20% and 30%, respectively, of present-day winter $PM_{2.5}$ composition in the North China Plain[37,38]. Nitrate $PM_{2.5}$ formation in China is generally limited by the supply of NO_x (refs. [40,41]), so a 9% decrease in NO_x emissions by 2020 would decrease $PM_{2.5}$ on average by about 1.8%. VOC reactivity for ozone formation in China is at present dominated by aromatics[42], whose emissions have increased rapidly over the past decade relative to other VOCs[43]. Aromatics are also a large source of organic $PM_{2.5}$ (refs. [44,45]). Assuming that 40% of organic $PM_{2.5}$ is secondary, that is, produced from the oxidation of VOCs[45,46], and that this component scales with VOC emissions[47], a 10% decrease in VOC emissions would decrease $PM_{2.5}$ by 1.2%. In this simple calculation, the 2018–2020 decreases of NO_x and VOC emissions planned under the Clean Air Action would result in a 3% decrease in $PM_{2.5}$, contributing substantially to the 8% $PM_{2.5}$ reduction goal while also improving ozone air quality. Further work should go beyond this

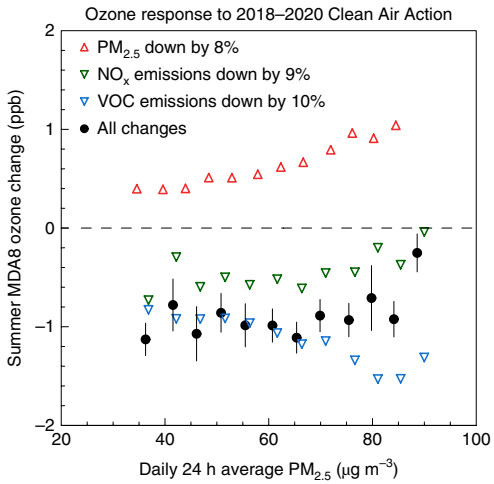

Fig. 4 | Expected ozone concentration change in the North China Plain under the 2018–2020 Clean Air Action plan. The figure shows mean MDA8 ozone responses in 5 μg m^{-3} $PM_{2.5}$ bins for the different changes projected by the 2018–2020 Clean Air Action plan relative to the 2017 GEOS-Chem baseline simulation. The changes are applied separately and then together ('All changes'). Values are regional averages for the North China Plain. The model data are sampled in the same way as in Fig. 1. Vertical bars for the 'All changes' simulation are the standard error on mean ozone for each bin.

simple estimate by examining $PM_{2.5}$ sensitivity to individual VOCs and the linearity of the response. Future research should also investigate the role of biogenic VOCs, which interact with the formation of anthropogenic $PM_{2.5}$ (refs. [48–50]), and whose emissions would be sensitive to changes in land use and climate[51].

In summary, we have shown through analysis of observed ozone–$PM_{2.5}$ relationships in China and supporting model simulations that ozone production is suppressed under high $PM_{2.5}$ conditions ($PM_{2.5}$ > 60 μg m^{-3}) because of $PM_{2.5}$ chemistry involving reactive uptake of both HO_x and NO_x radicals. Ozone concentrations in the North China Plain are reduced by about 25 ppb relative to $PM_{2.5}$-free conditions when $PM_{2.5}$ exceeds 80 μg m^{-3}. $PM_{2.5}$ chemistry results in ozone production that is more VOC-limited than it otherwise would be, emphasizing the importance of controlling reactive VOC emissions to abate ozone pollution in China. The 2018–2020 Clean Air Action plan of the Chinese government calls for a 10% decrease in VOC emissions; we find that this should offset the effect on ozone of the continued decrease in $PM_{2.5}$ concentrations, reversing the trend of increasing ozone. More aggressive VOC emission controls would further decrease ozone concentrations. With organic and nitrate $PM_{2.5}$ now contributing a large share of total $PM_{2.5}$, controlling VOC and NO_x emissions would substantially improve both $PM_{2.5}$ and ozone air quality.

Online content

Any methods, additional references, Nature Research reporting summaries, source data, statements of code and data availability and associated accession codes are available at https://doi.org/10.1038/s41561-019-0464-x.

Received: 14 May 2019; Accepted: 4 September 2019;
Published online: 14 October 2019

References

1. Chen, S. Q. et al. *The Sixth Assessment on Air Quality: Regional Air Pollution in "2+43" Cities during 2013–2018* (in Chinese) (Peking University, 2019); http://www.gsm.pku.edu.cn/pdf/2013201820190410.pdf
2. Silver, B., Reddington, C. L., Arnold, S. R. & Spracklen, D. V. Substantial changes in air pollution across China during 2015–2017. *Environ. Res. Lett.* **13**, 114012 (2018).
3. Liu, H. et al. Ground-level ozone pollution and its health impacts in China. *Atmos. Environ.* **173**, 223–230 (2018).
4. *Action Plan on Air Pollution Prevention and Control* (in Chinese) (Chinese State Council, 2013); http://www.gov.cn/zwgk/2013-09/12/content_2486773.htm
5. Huang, J., Pan, X., Guo, X. & Li, G. Health impact of China's Air Pollution Prevention and Control Action Plan: an analysis of national air quality monitoring and mortality data. *Lancet Planet. Health* **2**, 313–323 (2018).
6. Zhai, S. X. et al. Fine particulate matter ($PM_{2.5}$) trends in China, 2013–2018: separating contributions from anthropogenic emissions and meteorology. *Atmos. Chem. Phys.* **19**, 11031–11041 (2019).
7. Lu, X. et al. Severe surface ozone pollution in China: a global perspective. *Environ. Sci. Technol. Lett.* **5**, 487–494 (2018).
8. Malley, C. S. et al. Updated global estimates of respiratory mortality in adults ≥30 years of age attributable to long-term ozone exposure. *Environ. Health Perspect.* **125**, 087021 (2017).
9. Yue, X. et al. Ozone and haze pollution weakens net primary productivity in China. *Atmos. Chem. Phys.* **17**, 6073–6089 (2017).
10. Avnery, S., Mauzerall, D. L., Liu, J. & Horowitz, L. W. Global crop yield reductions due to surface ozone exposure: 1. Year 2000 crop production losses and economic damage. *Atmos. Environ.* **45**, 2284–2296 (2011).
11. Massey, S. W. The effects of ozone and NO_x on the deterioration of calcareous stone. *Sci. Total Environ.* **227**, 109–121 (1999).
12. Zheng, B. et al. Trends in China's anthropogenic emissions since 2010 as the consequence of clean air actions. *Atmos. Chem. Phys.* **18**, 14095–14111 (2018).
13. Wang, T. et al. Ozone pollution in China: a review of concentrations, meteorological influences, chemical precursors, and effects. *Sci. Total Environ.* **575**, 1582–1596 (2017).
14. Brasseur, G. P. & Jacob, D. J. *Modeling of Atmospheric Chemistry* (Cambridge Univ. Press, 2017).
15. Li, K. et al. Anthropogenic drivers of 2013–2017 trends in summer surface ozone in China. *Proc. Natl Acad. Sci. USA* **116**, 422–427 (2019).
16. Russell, A. et al. Urban ozone control and atmospheric reactivity of organic gases. *Science* **269**, 491–495 (1995).
17. Cohan, D. S., Hakami, A., Hu, Y. & Russell, A. G. Nonlinear response of ozone to emissions: source apportionment and sensitivity analysis. *Environ. Sci. Technol.* **39**, 6739–6748 (2005).
18. Jin, X. M. & Holloway, T. Spatial and temporal variability of ozone sensitivity over China observed from the Ozone Monitoring Instrument. *J. Geophys. Res. Atmos.* **120**, 7229–7246 (2015).
19. Schnell, J. L. & Prather, M. J. Co-occurrence of extremes in surface ozone, particulate matter, and temperature over eastern North America. *Proc. Natl Acad. Sci. USA* **114**, 2854–2859 (2017).
20. Zhu, J., Chen, L., Liao, H. & Dang, R. Correlations between $PM_{2.5}$ and ozone over China and associated underlying reasons. *Atmosphere* **10**, 352 (2019).
21. Fiore, A. M. et al. Background ozone over the United States in summer: origin, trend, and contribution to pollution episodes. *J. Geophys. Res.* **107**, 4275 (2002).
22. Xing, J. et al. Impacts of aerosol direct effects on tropospheric ozone through changes in atmospheric dynamics and photolysis rates. *Atmos. Chem. Phys.* **17**, 9869–9883 (2017).
23. Hollaway, M. et al. Photochemical impacts of haze pollution in an urban environment. *Atmos. Chem. Phys.* **19**, 9699–9714 (2019).
24. Jacob, D. J. Heterogeneous chemistry and tropospheric ozone. *Atmos. Environ.* **34**, 2131–2159 (2000).
25. Abbatt, J. P., Lee, A. K. & Thornton, J. A. Quantifying trace gas uptake to tropospheric aerosol: recent advances and remaining challenges. *Chem. Soc. Rev.* **41**, 6555–6581 (2012).
26. Taketani, F. et al. Measurement of overall uptake coefficients for HO_2 radicals by aerosol particles sampled from ambient air at Mts. Tai and Mang (China). *Atmos. Chem. Phys.* **12**, 11907–11916 (2012).
27. Mao, J., Fan, S., Jacob, D. J. & Travis, K. R. Radical loss in the atmosphere from Cu-Fe redox coupling in aerosols. *Atmos. Chem. Phys.* **13**, 509–519 (2013).
28. Jaeglé, L. et al. Nitrogen oxides emissions, chemistry, deposition, and export over the Northeast United States during the WINTER aircraft campaign. *J. Geophys. Res. Atmos.* **123**, 12368–12393 (2018).
29. Sillman, S., Logan, J. A. & Wofsy, S. C. The sensitivity of ozone to nitrogen oxides and hydrocarbons in regional ozone episodes. *J. Geophys. Res.* **95**, 1837–1852 (1990).
30. Kleinman, L. I. Low and high NO_x tropospheric photochemistry. *J. Geophys. Res. Atmos.* **99**, 16831–16838 (1994).
31. Jacob, D. J. et al. Seasonal transition from NO_x- to hydrocarbon-limited conditions for ozone production over the eastern United States in September. *J. Geophys. Res. Atmos.* **100**, 9315–9324 (1995).

32. Sillman, S. The use of NO_y, H_2O_2, and HNO_3 as indicators for ozone-NO_x-hydrocarbon sensitivity in urban locations. *J. Geophys. Res. Atmos.* **100**, 14175–14188 (1995).
33. Lu, C. H. & Chang, J. S. On the indicator-based approach to assess ozone sensitivities and emissions features. *J. Geophys. Res. Atmos.* **103**, 3453–3462 (1998).
34. Martin, R. V., Fiore, A. M. & van Donkelaar, A. Space-based diagnosis of surface ozone sensitivity to anthropogenic emissions. *Geophys. Res. Lett.* **31**, L06120 (2004).
35. Campbell, P. et al. A multi-model assessment for the 2006 and 2010 simulations under the Air Quality Model Evaluation International Initiative (AQMEII) phase 2 over North America: Part I. Indicators of the sensitivity of O_3 and $PM_{2.5}$ formation regimes. *Atmos. Environ.* **115**, 569–586 (2015).
36. Zhao, L. et al. Changes of chemical composition and source apportionment of $PM_{2.5}$ during 2013–2017 in urban Handan, China. *Atmos. Environ.* **206**, 119–131 (2019).
37. Huang, X. J. et al. Chemical characterization and source identification of $PM_{2.5}$ at multiple sites in the Beijing–Tianjin–Hebei region, China. *Atmos. Chem. Phys.* **17**, 12941–12962 (2017).
38. Sun, X. Y. et al. More recognized causes of severe haze pollution in Beijing-Tianjin-Hebei and surrounding areas (in Chinese). *People's Daily* http://paper.people.com.cn/rmrb/page/2019-03/21/07/rmrb2019032107.pdf (21 March 2019).
39. *Three-Year Action Plan on Defending the Blue Sky* (in Chinese) (Chinese State Council, 2018); http://www.gov.cn/zhengce/content/2018-07/03/content_5303158.htm
40. Liu, M. et al. Ammonia emission control in China would mitigate haze pollution and nitrogen deposition, but worsen acid rain. *Proc. Natl Acad. Sci. USA* **116**, 7760–7765 (2019).
41. Xu, Z. et al. High efficiency of livestock ammonia emission controls in alleviating particulate nitrate during a severe winter haze episode in northern China. *Atmos. Chem. Phys.* **19**, 5605–5613 (2019).
42. Wu, R. & Xie, S. Spatial distribution of ozone formation in China derived from emissions of speciated volatile organic compounds. *Environ. Sci. Technol.* **51**, 2574–2583 (2017).
43. Li, M. et al. Persistent growth of anthropogenic non-methane volatile organic compound (NMVOC) emissions in China during 1990–2017: drivers, speciation and ozone formation potential. *Atmos. Chem. Phys.* **19**, 8897–8913 (2019).
44. Guo, H. et al. Tropospheric volatile organic compounds in China. *Sci. Total Environ.* **574**, 1021–1043 (2017).
45. Huang, R. J. et al. High secondary aerosol contribution to particulate pollution during haze events in China. *Nature* **514**, 218–222 (2014).
46. Tong, K. N. The top scientific research teams provide pollution control guidance, and support to defend the blue sky battle (in Chinese). *The Paper* https://www.thepaper.cn/newsDetail_forward_3246478 (2019).
47. Hodzic, A. & Jimenez, J. L. Modeling anthropogenically controlled secondary organic aerosols in a megacity: a simplified framework for global and climate models. *Geosci. Model Dev.* **4**, 901–917 (2011).
48. Marais, E. A. et al. Aqueous-phase mechanism for secondary organic aerosol formation from isoprene: application to the southeast United States and co-benefit of SO_2 emission controls. *Atmos. Chem. Phys.* **16**, 1603–1618 (2016).
49. Fisher, J. A. et al. Organic nitrate chemistry and its implications for nitrogen budgets in an isoprene- and monoterpene-rich atmosphere: constraints from aircraft (SEAC^{4}RS) and ground-based (SOAS) observations in the Southeast US. *Atmos. Chem. Phys.* **16**, 2961–2990 (2016).
50. Pye, H. O. T. et al. On the implications of aerosol liquid water and phase separation for organic aerosol mass. *Atmos. Chem. Phys.* **17**, 343–369 (2017).
51. Guenther, A. et al. The Model of Emissions of Gases and Aerosols from Nature version 2.1 (MEGAN2.1): an extended and updated framework for modeling biogenic emissions. *Geosci. Model Dev.* **5**, 1471–1492 (2012).

Acknowledgements

This work is a contribution from the Harvard–NUIST Joint Laboratory for Air Quality and Climate. H.L. is supported by National Natural Science Foundation of China Grant 91744311. We thank China's Ministry of Ecology and Environment for running the nationwide observation network and publishing hourly concentrations of air pollutants.

Author contributions

K.L. and D.J.J. conceived the study. K.L. performed the analysis. H.L., J.Z., V.S., L.S. and S.Z. contributed to interpreting the data. V.S. and K.H.B. helped with model simulations. Q.Z. provided emission data. K.L. wrote the draft of the paper with D.J.J. and H.L. All authors contributed to discussing and improving the paper.

Competing interests

The authors declare no competing interests.

Additional information

Supplementary information is available for this paper at https://doi.org/10.1038/s41561-019-0464-x.

Correspondence and requests for materials should be addressed to D.J.J. or H.L.

Peer review information Primary Handling Editor(s): Heike Langenberg.

Reprints and permissions information is available at www.nature.com/reprints.

Publisher's note Springer Nature remains neutral with regard to jurisdictional claims in published maps and institutional affiliations.

Methods

Observations. Hourly surface air ozone and $PM_{2.5}$ concentrations for summer (June–August) 2013–2018 were obtained from the public website of the MEE. We focused on the four megacity clusters targeted by the Clean Air Action: North China Plain (34°–40° N, 114°–118° E, 106 sites), Yangtze River Delta (30°–33° N, 119°–122° E, 84 sites), Pearl River Delta (21.5°–24° N, 112°–115.5° E, 66 sites) and Sichuan Basin (28.5°–31.5° N, 103.5°–107° E, 71 sites). See Supplementary Fig. 1 for the geographical domains. We calculated daily MDA8 ozone and 24 h $PM_{2.5}$ concentrations at individual sites and averaged them over the megacity clusters.

Rigorous analysis of the observed ozone–$PM_{2.5}$ relationships in terms of ozone suppression under high $PM_{2.5}$ conditions (Fig. 1a) must correct for the effect of the 2013–2018 trends driven by changes in emissions[6,12,15], because these emission-driven trends (decreases in $PM_{2.5}$, increases in ozone) would otherwise produce a negative relationship between the two. We have argued previously that the 2013–2018 increase in ozone is driven mostly by the decrease in $PM_{2.5}$, but other factors, including trends in NO_x emissions and meteorology, could also play a role[15]. Here we detrended the time series for ozone and $PM_{2.5}$ by removing the ordinary linear regressions of daily concentrations versus time for each megacity cluster over the 2013–2018 period and then adding back the 2013–2018 mean concentrations. The data without detrending show an even stronger suppression of ozone under high-$PM_{2.5}$ conditions (Supplementary Fig. 5).

Chemical transport model simulations. GEOS-Chem simulations for 2016–2017 over the East Asia domain (including all of China and adjacent regions) were conducted with the nested-grid version of the model (version 12.0.0; http://www.geos-chem.org/). The model configuration is the same as in ref. [15] except for minor updates to HO_2 and NO_x uptake by PM (see the following paragraph). The model includes detailed ozone–NO_x–VOC–PM–halogen tropospheric chemistry[52,53] and is driven by meteorological data from the NASA Modern-Era Retrospective Analysis for Research and Applications, Version 2 (MERRA-2) (https://gmao.gsfc.nasa.gov/reanalysis/MERRA-2). The model's horizontal resolution is 0.5° × 0.625°, following the grid of the MERRA-2 data. Chemical boundary conditions at the edges of the East Asia domain are updated every 3 h from a 4° × 5° global simulation. The GEOS-Chem simulation of surface ozone in China has been evaluated in a number of previous studies[15,54–56]. In ref. [15], we showed that the model can reproduce the observed ozone distribution across China in summer with no notable bias.

$PM_{2.5}$ affects ozone in GEOS-Chem by perturbing the radiation field (and hence photolysis rates) and by providing surfaces for reactive uptake. Effects on photolysis rates are computed with the Fast-JX radiative transfer code of ref. [57] as implemented in GEOS-Chem by refs. [58,59]. The HO_2 reactive uptake coefficient (γ_{HO_2}) in GEOS-Chem is 0.2, producing either H_2O or H_2O_2 (refs. [24,27]). Here we set H_2O_2 as a product, following refs. [24,53], unlike ref. [15], which set H_2O as a product, but the choice of product has no notable effect on the ozone simulation[15]. Reactive uptake coefficients for N_2O_5, NO_2 and NO_3 are updated from GEOS-Chem version 12.0.0 on the basis of recent work by refs. [28,60]. This includes the parameterization of $\gamma_{N_2O_5}$ for converting N_2O_5 to HNO_3 on sulfate–nitrate–ammonium $PM_{2.5}$ (ref. [61]) and organic $PM_{2.5}$ (ref. [62]), $\gamma_{NO_2} = 1 \times 10^{-5}$ for conversion of NO_2 to HONO and HNO_3 (which yields a good simulation of HONO/NO_2 concentration ratios in China[60]) and $\gamma_{NO_3} = 1 \times 10^{-3}$ for conversion of NO_3 to HNO_3 (ref. [24]).

Anthropogenic emissions are from MEIC (http://www.meicmodel.org/)[12] and from MIX Asian emission inventory[63] for other Asian countries. Open fire emissions are from the Global Fire Emissions Database version 4 (ref. [64]). Natural emissions include NO_x from lightning[65] and soil[66], and biogenic emissions of VOC from vegetation calculated according to the Model of Emissions of Gases and Aerosols from Nature version 2 (ref. [51]).

A number of GEOS-Chem sensitivity simulations were carried out for this work, as listed in Supplementary Table 1 and described below. All reported results are after a one-month initialization.

Ozone–$PM_{2.5}$ relationship. We conducted sensitivity simulations removing the effects of $PM_{2.5}$-induced changes in photolysis rates, reactive uptake of HO_2 and reactive uptake of NO_x (as N_2O_5, NO_2 and NO_3). Each was first removed separately, and then all were removed concurrently. The changes in $PM_{2.5}$ were applied only to the boundary layer below 1.3 km (ref. [67]) to avoid changes in the ozone background.

Sensitivity to NO_x and VOC emissions. We conducted sensitivity simulations for 2017 with uniform 10%, 20%, 30%, 40% and 50% decreases of anthropogenic NO_x or VOC emissions relative to the baseline simulation. We repeated the same ensemble of simulations without $PM_{2.5}$ effects below 1.3 km altitude.

Effectiveness of 2018–2020 Clean Air Action plan. We conducted sensitivity simulations relative to the 2017 baseline simulation by applying a uniform 9% decrease of anthropogenic NO_x emissions over China, a 10% decrease of anthropogenic VOC emissions and an 8% decrease of $PM_{2.5}$ concentrations, first separately and then together.

Data availability

The surface measurements for $PM_{2.5}$ and ozone from China's Ministry of Ecology and Environment can be downloaded from beijingair.sinaapp.com. The anthropogenic emission inventory is available from www.meicmodel.org. The MERRA-2 reanalysis data are from https://gmao.gsfc.nasa.gov/reanalysis/MERRA-2. The GEOS-Chem simulation results are available from the corresponding authors on request

Code availability

The GEOS-Chem model code is open source (https://doi.org/10.5281/zenodo.2658178). Code for calculation and data processing is available from the corresponding authors on request.

References

52. Sherwen, T. et al. Global impacts of tropospheric halogens (Cl, Br, I) on oxidants and composition in GEOS-Chem. *Atmos. Chem. Phys.* **16**, 12239–12271 (2016).
53. Travis, K. R. et al. Why do models overestimate surface ozone in the southeastern United States? *Atmos. Chem. Phys.* **16**, 13561–13577 (2016).
54. Zhu, J., Liao, H., Mao, Y., Yang, Y. & Jiang, H. Interannual variation, decadal trend, and future change in ozone outflow from East Asia. *Atmos. Chem. Phys.* **17**, 3729–3747 (2017).
55. Ni, R., Lin, J., Yan, Y. & Lin, W. Foreign and domestic contributions to springtime ozone over China. *Atmos. Chem. Phys.* **18**, 11447–11469 (2018).
56. Lu, X. et al. Exploring 2016–2017 surface ozone pollution over China: source contributions and meteorological influences. *Atmos. Chem. Phys.* **19**, 8339–8361 (2019).
57. Bian, H. & Prather, M. J. Fast-J2: accurate simulation of stratospheric photolysis in global chemical models. *J. Atmos. Chem.* **41**, 281–296 (2002).
58. Mao, J. et al. Chemistry of hydrogen oxide radicals (HO_x) in the Arctic troposphere in spring. *Atmos. Chem. Phys.* **10**, 5823–5838 (2010).
59. Eastham, S. D., Weisenstein, D. K. & Barrett, S. R. Development and evaluation of the unified tropospheric–stratospheric chemistry extension (UCX) for the global chemistry-transport model GEOS-Chem. *Atmos. Environ.* **89**, 52–63 (2014).
60. Shah, V. et al. Effect of changing NO_x lifetime on the seasonality and long-term trends of satellite-observed tropospheric NO_2 columns over China. *Atmos. Chem. Phys. Discuss.* (2019); https://www.atmos-chem-phys-discuss.net/acp-2019-670/acp-2019-670.pdf
61. Bertram, T. H. & Thornton, J. A. Toward a general parameterization of N_2O_5 reactivity on aqueous particles: the competing effects of particle liquid water, nitrate and chloride. *Atmos. Chem. Phys.* **9**, 8351–8363 (2009).
62. Badger, C. L., Griffiths, P. T., George, I., Abbatt, J. P. & Cox, R. A. Reactive uptake of N_2O_5 by aerosol particles containing mixtures of humic acid and ammonium sulfate. *J. Phys. Chem.* **110**, 6986–6994 (2006).
63. Li, M. et al. MIX: a mosaic Asian anthropogenic emission inventory under the international collaboration framework of the MICS-Asia and HTAP. *Atmos. Chem. Phys.* **17**, 935–963 (2017).
64. Van der Werf et al. Global fire emissions and the contribution of deforestation, savanna, forest, agricultural, and peat fires (1997–2009). *Atmos. Chem. Phys.* **10**, 11707–11735 (2010).
65. Murray, L. T., Jacob, D. J., Logan, J. A., Hudman, R. C. & Koshak, W. J. Optimized regional and interannual variability of lightning in a global chemical transport model constrained by LIS/OTD satellite data. *J. Geophys. Res.* **117**, D20307 (2012).
66. Hudman, R. C. et al. Steps towards a mechanistic model of global soil nitric oxide emissions: implementation and space based-constraints. *Atmos. Chem. Phys.* **12**, 7779–7795 (2012).
67. Guo, J. P. et al. The climatology of planetary boundary layer height in China derived from radiosonde and reanalysis data. *Atmos. Chem. Phys.* **16**, 13309–13319 (2016).